**Hydrology and Earth System Sciences Discussions**

**Hydrological responses to climate change conditioned by land-use**

J. Jarsjö et al.

| | |
|---|---|
| Title Page | |
| Abstract | Introduction |
| Conclusions | References |
| Tables | Figures |
| ◄◄ | ►► |
| ◄ | ► |
| Back | Close |
| Full Screen / Esc | |
| Printer-friendly Version | |
| Interactive Discussion | |

# Hydrological responses to climate change conditioned by historic alterations of land-use and water-use

**J. Jarsjö, S. M. Asokan, C. Prieto, A. Bring, and G. Destouni**

Department of Physical Geography and Quaternary Geology, Bert Bolin Centre for Climate Research, Stockholm University, 10691 Stockholm, Sweden

Correspondence to: J. Jarsjö (jerker.jarsjo@natgeo.su.se)

## Abstract

This paper quantifies and conditions expected hydrological responses in the Aral Sea Drainage Basin (ASDB; occupying 1.3 % of the earth's land surface), Central Asia, to multi-model projections of climate change in the region from 20 general circulation
5  models (GCMs). The aim is to investigate how uncertainties of future climate change interact with the effects of historic human re-distributions of water for land irrigation to influence future water fluxes and water resources. So far, historic irrigation changes have greatly amplified water losses by evapotranspiration (ET) in the ASDB, whereas the 20th century climate change has not much affected the regional net water loss to
10  the atmosphere. Projected future climate change (for the period 2010–2039) however is here calculated to considerably increase the net water loss to the atmosphere. Furthermore, the ET response strength to any future temperature change will be further increased by maintained (or increased) irrigation practices. With such irrigation practices, the river runoff is likely to decrease to near-total depletion, with risk for cascading
15  ecological regime shifts in aquatic ecosystems downstream of irrigated land areas. Without irrigation, the agricultural areas of the principal Syr Darya river basin could sustain a 50 % higher temperature increase (of 2.3 °C instead of the projected 1.5 °C until 2010–2039) before yielding the same consumptive ET increase and associated $R$ decrease as with the present irrigation practices.

## 1  Introduction

Human changes in land-use and water-use of the past century have considerably impacted the cycling of water and water-borne substances (Foley et al., 2005; Piao et al., 2007; Shibuo et al., 2006; Weiskel et al., 2007; Wisser et al., 2010). In particular, re-distribution of freshwater for irrigation of extensive agricultural areas (Asokan et al.,
25  2010; Destouni et al., 2010; Lee et al., 2011; Lobell et al., 2009; Shibuo et al., 2007; Törnqvist and Jarsjö, 2011) has increased net water fluxes from the land surface to

the atmosphere by about 2000 km$^3$ per year, which constitutes the major part of the total human freshwater withdrawals (Foley et al., 2005; Gordon et al., 2005). Except for deforestation (Gordon et al., 2005), no other human modification has so far affected water fluxes to such an extent. These freshwater changes are significant and influence
5  socio-economic development in most parts of the world. For instance, close to one billion people live in regions where agricultural yields have been much enhanced by irrigation (Keiser et al., 2005; Lobell and Field, 2007). Whereas agricultural efficiency needs to increase in order to decrease malnutrition and support a growing population, current high-yield agriculture is dependent on irrigation, fertilization and pest control,
10  which is associated with degradation of environmental resources from salinization, contamination, and water logging (Gordon et al., 2008; Johansson et al., 2009; Törnqvist et al., 2011).

In order to realistically plan for land-use and water-use changes, and efficiently mitigate the adverse effects of such changes, processes need to be understood and quan-
15  tified on the drainage basin scale. This is best done within hydrological basins, because the topographical water divides that define these basins are physical boundaries that reasonably well delimit the flows of water and water-borne substances through the landscape, and the environmental impacts of man-made changes to these flows. Existence of large aquifer systems means that groundwater flows may extend over larger
20  hydrological units than surface water basins. However, these subsurface flow effects decrease with increasing basin scale and can in many cases be investigated and quantified by state-of-the -art hydrogeological methods. The increasing hydrological impacts of climate change (Bengtsson, 2010; Groves et al., 2008; Milly et al., 2005) constitute a greater quantification challenge, with several open scientific questions in need of fur-
25  ther investigation, not least regarding the large spatial scale discrepancy between a typical drainage basin and its hydrological modeling, and the global scale and coarse resolution of general circulation models (GCMs) (Groves et al., 2008; Milly et al., 2005).

Furthermore, available high-quality observational data series for most hydrological basins are often too short to capture the long-term effects of relatively slow changes

in land-use, water-use and climate, making it difficult to validate the long-term change performances of hydro-climatic models. It is such slow boundary condition changes – rather than particular hydrological events – that drive long-term change in hydrological system characteristics. Modeling of the latter does not depend on given initial condi-
5  tions, such as the particular surface and ground water levels, and soil moisture conditions at simulation start, in contrast to modeling of short-term hydrological variability, such as stream flow responses to rainfall events, the model results of which do depend on the initial hydrological conditions. This fundamental modeling difference between long-term hydrological change and short-term hydrological variability is analogous to
10  projections of climate change (that is, change in long-term weather characteristics) over a multi-decadal GCM-run being independent of given initial weather conditions at simulation start.

Regionally, the impacts on water resources from changes in global atmospheric circulation and climate overlap with the impacts from land-use and water-use changes
15  (Lobell and Field, 2007). For instance, in arid and semi-arid regions, water availability critically limits water-demanding agricultural expansion and economic growth, making such regions particularly vulnerable to impacts of expected future climate changes (IPCC, 2007). The different overlapping causes of freshwater resource changes make it hard to distinguish between various hydrological cause-effect relations and impacts
20  (Destouni et al., 2008; Milly et al., 2002; Piao et al., 2007). However, for all water resource changes that are driven by different change pressures at the surface of a hydrological basin, hydro-climatic change projections can be considerably improved by honoring and accounting for the water flux bounds implied by the basic basin-scale water balance equation $ET = P - R - \Delta S$. Such bounds on the commonly difficult to
25  measure and quantify vapour flux by evapotranspiration (ET) at the land surface can then be derived on basin scales from directly measured and/or model-interpreted data on precipitation ($P$) at the basin surface, runoff ($R$) at the basin outlet, and storage change ($\Delta S$) within the basin (Asokan et al., 2010; Destouni et al., 2010; Shibuo et al., 2007; Törnqvist and Jarsjö, 2011).

In this paper, we use and extend (from previous related studies of historic hydro-climatic change; Alekseeva et al., 2009; Destouni et al., 2010; Shibuo et al., 2007; Törnqvist and Jarsjö, 2011) such a basin-scale water balance approach to investigate future hydrological responses to projected climate change at the land surface of a hydrological basin. This is done by linking the projections of basin-scale surface climate change from 20 different GCMs with already developed hydrological modeling (based on the above-cited historic hydro-climatic change studies and data) for the example case of the closed and intensely irrigated Aral Sea Drainage Basin (ASDB) in Central Asia. The ASDB is one of the world's largest hydrological basins and is spatially well resolved by current GCMs. Furthermore, the dramatic Aral Sea shrinkage over the last 60 years constitutes a great amplifier of different water change signals, which has been used in previous water balance-based studies of the ASDB to understand and resolve the historic impacts of different hydro-climatic change drivers in this basin. A main question investigated here is then to what extent, and how, future climate change can interact with the human re-distributions of water in modifying future water fluxes and impacting future water resource availability. Such interactions with local-regional water resource management are not well resolved in current GCMs, or in regional climate models (RCMs). To complement such large-scale modeling, the present basin-scale water balance approach can explicitly consider and account for how various hydrological flows, such as ET, are limited by actual basin-scale human water and resulting water availability. We also investigate and provide example quantifications of main uncertainties in such modeling of hydrological responses to multi-GCM projections of future basin-scale climate change.

## 2 Study area and historic hydro-climatic change

We here analyze surface boundary-driven, multi-decadal hydrological changes, following the historic 20th century development of approximately 8 million hectares of irrigated land in the ASDB. With its total area of $1\,870\,000\,\text{km}^2$, the ASDB occupies 1.3 %

of the Earth's land surface, and by its traditional definition, almost the entire region of Central Asia (Fig. 1). Records of hydrological responses to the historic changes in surface boundary conditions show that, despite a $P$ increase from the beginning of the 20th century (Fig. 1), the discharge ($Q$) into the Aral Sea, through the principal rivers
5 of Amu Darya and Syr Darya in the ASDB, has decreased from the pre-1950 value of about 60 km$^3$ yr$^{-1}$ to today's average of less than 10 km$^3$ yr$^{-1}$ (Destouni et al., 2010; Jarsjö and Destouni, 2004; Shibuo et al., 2007). Such a $Q$ decrease may in principle be associated with a corresponding increase in the water vapor flux to the atmosphere through ET, or in the groundwater recharge and associated diffuse groundwater dis-
10 charges (DD) to the Aral Sea, or some combination of both. The fate of the missing water associated with a decrease in river discharge $Q$ must be estimated independently in order to resolve how much of the so far observed $Q$ change reflects an ET change, and how much should be attributed to a DD change.

In the ASDB, all diffuse groundwater flow converges into the terminal Aral Sea, con-
15 tributing to its water level, which has decreased by 25 m since the 1960's. Detailed previous water balance studies with a coupled groundwater-seawater model and in-dependent analyses of groundwater hydraulics have shown that this decrease is in-compatible with large increases in DD (Alekseeva et al., 2009; Jarsjö and Destouni, 2004; Shibuo et al., 2006). Since the historic changes in DD are much smaller than
20 the observed historic $Q$ changes in the ASDB, the latter must be due to ET changes of corresponding magnitude. Previously reported ASDB results have further shown that the ET losses associated with the historic, post-1950 temperature ($T$) increase of 1 °C (Fig. 1a) are smaller than the historic water gains from increased $P$ (Fig. 1b), and that the drying of ASDB rivers ($Q$ decrease) and associated major Aral Sea shrinkage have
25 not so far been driven by the observed historic surface climate change within the ASDB (Shibuo et al., 2007).

## 3   Future hydro-climatic change projections

We consider future climate change scenarios for the ASDB (Fig. 1) by using the spatially distributed outputs for this basin from 20 General Circulation Models (GCMs). These comprise all available GCMs in the third and fourth assessment reports (TAR and AR4, respectively; Greenhouse Gas Emission Scenario A2a) of the Intergovernmental Panel of Climate Change (IPCC) (IPCC, 2007), from which both $T$ and $P$ output is available. As the ASDB extends over a considerable number of grid cells ($29 \pm 23$) of the considered GCMs (Table 1), the GCM spatial resolution biases should be small (Milly et al., 2005; Mujumdar and Ghosh, 2008; Wood et al., 2004), justifying hydrological impact studies by direct use of GCM projection results for basins of this size (Milly et al., 2002; Palmer and Räisänen, 2002).

### 3.1   Catchment delineation and hydrological modeling steps

The hydrological modeling considered here is spatially distributed, using the water module of the PCRaster-based Polflow model (De Wit, 2001), similarly to previous investigations of historic hydro-climatic variability and change, specifically for the ASDB (Shibuo et al., 2007) as well as for other drainage basins in different parts of the world (Asokan et al., 2010; Darracq et al., 2005; Darracq and Destouni, 2009; Jarsjö et al., 2008). More specifically, the topography-driven flow network of the ASDB was constructed based on Shuttle Radar Topography Mission (SRTM) data (Farr et al., 2007), isobath data from Alekseeva et al. (2009), and stream location data from the Digital Chart of the World (Danko, 1992). Using PCRaster/ PolFlow routines (De Wit, 2001) the ASDB delineation was made from the sum of all the upstream catchment areas associated with all discharge outlet points along the whole Aral Sea coastline. In analogy, the total discharge into the Aral Sea was given by the sum of all the outlet discharges along its coastline, and the Amu Darya and Syr Darya river discharges were estimated at their respective outlet points at the Aral Sea. We followed the same detailed procedures as in Shibuo et al. (2007).

As input for the hydrological modeling module in PCRaster/PolFlow, each of the 9 million cells of the hydrological grid was assigned properties of ground slope and slope direction (based on the SRTM data), precipitation P and temperature T (30-year average from GCM output or observational data from the Climate Research Unit TS 2.1 database (Mitchell and Jones, 2005), and land use (classified as irrigated or not irrigated, from the Global Map of Irrigated Areas; Siebert et al., 2005). The total river discharge ($Q$) and total runoff ($R$) leaving a model pixel was calculated by the network-routed sum of locally created average precipitation surplus, PS. For each grid cell, PS was calculated as $P$ – ET, where the actual evapotranspiration (ET) was estimated from the potential evapotranspiration $ET_a$ according to Turc (1954), with $ET_p$ estimated as a function of $T$ according to Langbein (1949). In the present as in previously reported results from distributed hydrological modeling of the ASDB (Destouni et al., 2010; Shibuo et al., 2007) and elsewhere (Asokan et al., 2010), irrigation has been handled by spreading the known water diversions from rivers (currently $50\,\text{km}^3\,\text{yr}^{-1}$ from the ASDB rivers) over the known irrigated areas in the basin.

## 3.2 Quantification of multi-decadal hydro-climatic change

The above-described hydrological model has previously been applied to both pre-irrigation conditions (without major water re-routings, i.e. before the 1950's), and current conditions (with present water diversions to irrigated fields) in the ASDB. Comparison with measurements showed that the modeling could independently reproduce the observed long-term changes in river discharge, implying that it is fully consistent with effects of historical, multi-decadal land-use and water-use driven changes in ASDB, the occurrence of which has so far greatly changed hydrological fluxes and water balances in the ASDB (Alekseeva et al., 2009; Destouni et al., 2010; Shibuo et al., 2007; Törnqvist and Jarsjö, 2011). Shibuo et al. (2007) also investigated to what extent model performance in reproducing observed multi-decadal changes of ASDB could be further enhanced by use of monthly hydro-climatic data as input to ET quantifications

by the Thornthwaite (1948) method. They found the latter to be similar and equally consistent with independent observations as the here-adopted Langbein (1949) ET method. Similar observation-consistent ET model results were also obtained between the Thornthwaite and Langbein methods under quite different multi-decadal water and
5 climate change conditions in the Mahanadi River Basin of western India (Asokan et al., 2010), with the ET and $R$ results of the two models differing by at most 3 %. Based on these previous ET model results for both the ASDB and other world parts, we do not also repeat the same ET model sensitivity exercise in the present quantifications.

For hydrological model results that account for irrigation, the irrigation and associated
10 engineered water diversions are assumed maintained at their current states also in the near future (2010–2039). This makes it possible to evaluate the hydrological responses to projected climate changes in a basin that is already under considerable pressure from irrigation. Despite plans for possible continued irrigation expansion in the upper parts of ASDB (Rakhmatullaev et al., 2010), the present stable irrigation assumption is
15 consistent with the acute regional water scarcity in Central Asia effectively prohibiting any actual further irrigation expansion in the lower basin parts (Törnqvist and Jarsjö, 2011). We further evaluate possible climate-irrigation interaction effects by calculating and comparing the different hydrological responses to projected climate change under an irrigation scenario (extending present irrigation conditions to the future) and a non-
20 irrigation scenario (taking possible future irrigation halting to the limit of zero irrigation), as detailed below.

Furthermore, because GCM bias effects on the modeling of hydrological fluxes, such as runoff, are uncertain, two alternative approaches are used to calculate future responses to climate change projections. Specifically, hydrological simulation results for
25 the reference period 1961–1990 are based on (i) direct output from GCM simulations, and (ii) CRU observational data. Results for the future period 2010–2039 are then based on adding the GCM change projections to (I) the GCM output for the reference period 1961–1990, and (II) the CRU observational data for 1961–1990. We call case (i) and (I) results uncalibrated, since they are based only on GCM output, and case (ii)

**Hydrological responses to climate change conditioned by land-use**

J. Jarsjö et al.

Full Screen / Esc

Printer-friendly Version

Interactive Discussion

and (II) results calibrated, since they are fitted to observational data for 1961–1990 (Fig. 1).

For each of these GCM projection approaches I and II, the future climate-driven ET change ($\Delta$ET) response is quantified as the difference in ET between the projected climate of the period 2010–2039 and the climate of the reference period 1961–1990. The effect of future irrigation development on $\Delta$ET is further investigated by considering two different irrigation scenarios: one scenario with irrigation maintained at present level in the basin (yielding $\Delta ET_{irr}$), and one without any future irrigation (yielding $\Delta ET_{no-irr}$). Seeing from the simulation results for these two scenarios that the same projected T increase yields climate-driven future $\Delta ET_{no-irr} < \Delta ET_{irr}$, the $T$ increase needed to obtain $\Delta ET_{no-irr} = \Delta ET_{irr}$ is finally also estimated by adding small, uniform increases to the initial $T$ distribution of the entire ASDB in the model scenario without irrigation, until a match of $\Delta ET_{irr}$ is obtained with the $\Delta ET_{no-irr}$ scenario.

## 4 Results

Observation data for $T$ from the Climate Research Unit (CRU) TS 2.1 (grey line in Fig. 1a) show an average $T$ value of 8.1 °C within the ASDB (shaded in the upper right, overview panel of Fig. 1) for the reference period 1961–1990. The $T$ output of the 14 GCMs used in AR4 (colored, thin lines of Fig. 1a; the IDs of the different GCMs are given as in Solomon et al., 2007) show relatively large individual discrepancies from this observation, with for instance the average $T$ for the reference period ranging between 4.6 and 11.4 °C. The corresponding ensemble mean value (of 7.9 °C), however, is close to the observed average $T$. The projected $T$ increase ($\Delta T$) for ASDB is also relatively consistent between the different GCMs, yielding an average future T for the period 2010–2039 that is 1.5 °C higher than $T$ for the reference period 1961–1990 (Fig. 1).

The AR4 model ensemble average $P$ value of 353 mm yr$^{-1}$ is considerably higher than the average $P$ of 257 mm yr$^{-1}$, based on $P$ observation data from CRU, for the reference period 1961–1990 (Fig. 1b). Furthermore, the two GCMs that give $P$-values

closest to observed $P$ (ECHAM4 and GIER) give $T$-values that are considerably above the observed $T$ (Fig. 1a), reflecting the fact that there is no single GCM that reasonably well reproduces both $P$ and $T$ for this large regional basin. Furthermore, the individual AR4 GCMs show quite different projected trends of $P$ change (decreasing, unchanged, or increasing), with the resulting model ensemble average value of future $P$ showing a slight increase of 10 mm yr$^{-1}$. The hydrological effects of differing future $P$ projections are then investigated here by adding the ensemble average $P$ change projection to: (I) the GCM ensemble average $P$ result for 1961–1990, or (II) the actually observed average $P$ for 1961–1990.

Mean results of the two approaches (I) and (II) for the TAR and AR4 GCM projections show that, with maintained irrigation practices, ET from the ASDB can be expected to increase by around 25 to 40 km$^3$ yr$^{-1}$ (Fig. 2). The difference between the uncalibrated and the calibrated ET results is much smaller for the AR4 (3.8 km$^3$ yr$^{-1}$) than for the TAR (10.2 km$^3$ yr$^{-1}$) GCM results, indicating improved hydro-climatic change precision in the AR4 GCMs. The AR4 GCM projections (Fig. 2a) yield further a slightly smaller average ET change than the TAR GCM projections (Fig. 2b). The runoff $R$, which expresses the net annual basin-scale water availability after $P$ reduction by ET, is then expected to decrease by between 5 and 15 km$^3$ yr$^{-1}$ due to the projected climate change between the periods 1961–1990 and 2010–2039 (Fig. 2). Such climate-driven near-future decreases in $R$ constitute a climate-effect trend break for the ASDB, as the climate-related $R$ change contribution experienced so far in this basin (with an average 1 °C $T$ increase trend for the last 50 years) has not yet contributed much to the total historic $R$ decrease to present conditions (Shibuo et al., 2007). Also for $R$, the AR4 GCMs yield smaller difference between calibrated and uncalibrated $R$ results (3.7 km$^3$ yr$^{-1}$) than the TAR GCMs (9.2 km$^3$ yr$^{-1}$). The consistency between the calibrated and uncalibrated results based on the GCM ensemble mean projections demonstrates that the GCM output uncertainties (particularly for AR4 GCMs) have relatively small influence on projected $R$ change trends for this region.

Title Page

Abstract | Introduction

Conclusions | References

Tables | Figures

◄ | ►|

◄ | ►

Back | Close

Full Screen / Esc

Printer-friendly Version

Interactive Discussion

The error bars in Fig. 2 show the standard deviation of the modeled ET change and $R$ change results based on the 14 AR4 (Fig. 2a) and 6 TAR (Fig. 2b) GCMs. These standard deviations are larger than the difference in ensemble mean results between both the TAR and AR4 models, and the calibrated and uncalibrated projection han-

5 dling approaches. This shows that hydrological modeling coupled to single GCMs can deviate considerably from corresponding ensemble mean results. In particular, a few individual GCM projections yield increasing $R$ (as can be understood from the fact that the corresponding standard deviations in Fig. 2 include zero values), in contrast to all four combinations of ensemble mean results (AR4-calibrated, AR4-uncalibrated, TAR-

10 calibrated and TAR-uncalibrated), which all yield decreasing $R$. Whereas the ensemble mean projections hence converge on yielding $R$ decrease results, the alternative approach of coupling hydrological modeling to a chosen single CGM can yield an opposing $R$ result, depending on the choice of GCM. This result also shows that the errors in $T$ and $P$ from single GCMs shown in Fig. 1 propagate critically to the main hydrologic

15 output parameter $R$. In the following two result figures, we therefore present ensemble mean results to avoid such error propagation from single GCM projections.

Table 2 summarizes the observational and GCM ensemble mean data of the climate parameters of Fig. 1, and shows the corresponding absolute values of the hydrological model output that underpin the change results presented in Fig. 2 (corresponding

20 standard deviations are shown in parenthesis). In particular, there is a large difference in absolute $R$ between the calibrated and uncalibrated approaches to GCM projection handling in the hydrological modeling. Without calibration, $R$ in the historic reference period (of $10 \, \mathrm{km}^3 \, \mathrm{yr}^{-1}$) is largely overestimated (by $135 - 10 = 125 \, \mathrm{km}^3 \, \mathrm{yr}^{-1}$ in the AR4 case; Table 2), mainly because the ensemble mean $P$ of the reference period is much

25 overestimated by the GCMs (solid red line; Fig. 1b). Notably, even though the absolute $R$-value of the uncalibrated modeling is more than 10 times too large, the associated result in terms of $R$-change is consistent with that from the calibrated modeling, as previously shown by the comparatively small difference between the red and blue bars in Fig. 2. The hydrological model results hence share this result characteristic with the

Title Page

Abstract | Introduction

Conclusions | References

Tables | Figures

◀ | ▶

◀ | ▶

Back | Close

Full Screen / Esc

Printer-friendly Version

Interactive Discussion

GCM projections, in which $T$ and $P$ change ($\Delta T$ and $\Delta P$) can be robust even though corresponding absolute values ($T$ and $P$) differ greatly between different GCMs and from observations.

For the ASDB, all multi-model projections converge on future climate change com-
5   bined with maintained irrigation practices leading to expected $R$ decrease, which can entirely deplete the principal rivers in this basin within the next 40 years (Fig. 3). This means that relatively small changes in future $T$ and $P$ can lead to relatively large changes in future river discharges. This is a non-linear $R$ response, considering that nearly equally large historic (20th century) $T$ and $P$ changes have so far yielded only
10  small $R$ change contributions (Destouni et al., 2010; Shibuo et al., 2007). This non-linearity is also seen in the significantly lower $R$ in the later (1984–1989) years of the reference period 1961–1990 (Fig. 3), despite the fact that $T$ and $P$ were the same in these later years as over the full reference period. It is this non-linearity in the $R$ response that will yield total or near-total future river depletion, which is in turn associated
15  with large risk for regime shifts in the aquatic ecosystems that depend on $R$ (Groves et al., 2008). This risk would not occur without the historic irrigation expansion that decreased the present $R$ so much (at least $50\,\mathrm{km}^3\,\mathrm{yr}^{-1}$ since the 1950's) and left it, and the associated freshwater resources, highly vulnerable to any further ambient change.

Moreover, maintaining the historically developed irrigation practices stable also in the
20  future will increase the hydrological ET sensitivity ($\Delta\mathrm{ET}/\Delta T$) to future climate change $\Delta T$, and hence increase the regional strength of the ET response to increasing temperature. Specifically, the same $\Delta T$ will drive a considerably greater $\Delta\mathrm{ET}$ with irrigation ($\Delta\mathrm{ET}_{\mathrm{irr}}$) than without it ($\Delta\mathrm{ET}_{\mathrm{no-irr}}$), as shown in Fig. 4a by the resulting difference $\Delta\mathrm{ET}_{\mathrm{irr}} - \Delta\mathrm{ET}_{\mathrm{no-irr}}$ for the GCM-projected ensemble mean $\Delta T$ of 1.5 °C for 2010–2039.
25  Figure 4b and c more generally illustrate the combined effects of $\Delta T$ and irrigation on $R$. Figure 4b (left panel) illustrates the straight-forward ET response (red arrows) to increasing $\Delta T$ in non-irrigated areas, resulting in a decrease of $R$ that corresponds to the increase of ET due only to $\Delta T$. The blue arrows in Fig. 4 illustrate ET under current climate conditions (without $\Delta T$), which is higher in areas with irrigation (Fig. 4c,

blue arrow) than without (Fig. 4b – left, blue arrows). The red arrows in Fig. 4b (left panel) and c show the ET response to the same $\Delta T = 1.5\,°C$ in non-irrigated and in irrigated areas, respectively. Comparison between Fig. 4b (right panel) and c finally illustrates that the agricultural areas along the Syr Darya river (the longest river in Central Asia) could without irrigation sustain a considerably higher temperature change, $\Delta T = 2.3\,°C$ (Fig. 4b – right), before yielding the same ET response as with the current irrigation practices and projected $\Delta T = 1.5\,°C$ (Fig. 4c). This implies a 50 % higher ET sensitivity to climate change with present irrigation practices than without any irrigation (i.e. $[\Delta ET_{irr}/\Delta T_{irr}]/[\Delta ET_{no-irr}/\Delta T_{no-irr}] = 2.3\,°C/1.5\,°C = 1.53$ for $\Delta ET_{irr} = \Delta ET_{no-irr}$). A direct consequence of increased ET sensitivity to $\Delta T$ is that the climate-driven future $R$ decrease is enhanced in irrigated areas, which may push downstream aquatic ecosystems closer to and beyond ecological regime shift thresholds.

## 5 Discussion

As found also in other studies (Rajagopalan et al., 2002), model-related biases in hydro-climatic change projections can be considerably reduced by use of multi-model ensemble mean outputs of a larger set of GCMs (as in AR4), instead of output from just a few (as in TAR) or single GCMs. The present hydrological model approaches to multi-GCM projection handling converge on showing that expected future $T$ and $P$ changes in the ASDB will decrease $R$ in the near-future period 2010–2039 considerably more with than without continued irrigation practices, due to the irrigation increase of ET and associated net losses of water from the basin to the atmosphere. These increased water losses may or may not be temporarily masked by runoff increases from internal water storage changes within the basin (e.g. caused by glacier melt; Radič and Hock, 2011).

More generally, a similar comparison of uncalibrated GCM results with observation data of $T$ and $P$, carried out by Bring and Destouni (2011) for major river basins in the hydro-climatically very different Arctic region, yielded consistent results with those

obtained here for the Central Asian ASDB. That is, ensemble mean GCM results represent observation data much better for $T$ than for $P$, and largely overestimate $P$ and its recent historic change so far for the Arctic region, similarly to the present Central Asian region of the ASDB. Furthermore, also for the Arctic, inter-GCM variability is larger for the (fewer) TAR than for the (considerably more) AR4 GCMs, implying greater precision, even though not much better accuracy with regard to $P$, for AR4.

The off-line, basin-scale water balance approach adopted here to the modeling of hydrological change responses to climate change implies that considerably refined hydrological routines (relative to the commonly very coarse hydrological process and result resolution in GCMs) can be coupled to a large number of GCMs (20 in the present case). Adopting a corresponding on-line approach for all different GCMs – i.e. implementing in each of them physically based and well-resolved hydrological routines that feed the regional hydrological model output back into the GCM and re-running it for all considered scenarios – would be a huge task. The alternative of implementing a corresponding on-line approach to a single chosen GCM can, for instance, provide more generic insights into the dynamics of feedback mechanisms. However, the current ASDB example illustrates that conclusions regarding even the direction of $R$ change (increasing or decreasing), drawn from a single GCM can contradict converging conclusions drawn from several, quite different multi-model approaches using ensemble mean GCM projections. Hence, results on the hydro-climatic development in ASDB can remain inconclusive if based on a single GCM. Based on the similar recent implications also for the very different Arctic region hydrology (Bring and Destouni, 2011), this is a conclusion that may hold true more generally for many of the world's hydrological basins, most of which are also considerably smaller than the ASDB, which increases GCM resolution biases and uncertainties relative to the ASDB.

The here quantified increase in ET (and associated $R$) response sensitivity to $T$ change with irrigation, relative to without it, implies more generally that global expansion of irrigation can considerably increase the adversity of future climate change effects on the world's water resources. It can also change the spatial distribution of

**Hydrological responses to climate change conditioned by land-use**

J. Jarsjö et al.

Title Page

Abstract | Introduction

Conclusions | References

Tables | Figures

|◄ | ►|

◄ | ►

Back | Close

Full Screen / Esc

Printer-friendly Version

Interactive Discussion

ET-related continental water feedbacks to climate change. Continued irrigation expansion planned by Central Asian states (Rakhmatullaev et al., 2010) may cause even greater ET losses and extend downstream river depletion in comparison to the case of maintained irrigation practices considered here. Water-efficient irrigation practices are needed to evade these more adverse climate change effects.

## 6  Conclusion summary

- All multi-model projections converge on showing that future climate change combined with maintained irrigation practices will lead to $R$ decreases that can entirely deplete the principal rivers in ASDB within the next 40 years.

- This total or near-total climate change-driven river depletion would not occur without the historic irrigation expansion that has so far decreased $R$ to its present low level.

- Without irrigation, the agricultural areas of the principal Syr Darya river basin could be subject to a 50 % higher temperature increase before yielding the same consumptive ET increase, and associated $R$ decrease, as with continued irrigation practices at present level.

- Conclusions drawn from single GCM projections regarding even the direction of future $R$ changes (increasing or decreasing) in the ASDB are not robust, i.e. single GCM projections can entirely contradict converging conclusions from quite different approaches to handling multi-GCM ensemble mean projections in hydrological modeling.

Title Page

Abstract | Introduction

Conclusions | References

Tables | Figures

|◄ | ►|

◄ | ►

Back | Close

Full Screen / Esc

Printer-friendly Version

Interactive Discussion

# References

Alekseeva, I., Jarsjö, J., Schrum, C., and Destouni, G.: Reproducing the Aral Sea water budget and sea-groundwater dynamics between 1979 and 1993 using a coupled 3-D sea-ice-groundwater model, J. Mar. Syst., 76, 296–309, 2009.

Asokan, S. M., Jarsjö, J., and Destouni, G.: Vapor flux by evapotranspiration: Effects of changes in climate, land use, and water use, J. Geophys. Res.-Atmos., 115, D24102, doi:10.1029/2010JD014417, 2010.

Bengtsson, L.: The global atmospheric water cycle, Environ. Res. Lett., 5, 025001, doi:10.1088/1748-9326/5/2/025001, 2010.

Bring, A. and Destouni, G.: Relevance of hydro-climatic change projection and monitoring for assessment of water cycle changes in the Arctic, Ambio, 40, 361–369, doi:10.1007/s13280-010-0109-1, 2011.

Danko, D. M.: The digital chart of the world project, Photogramm. Eng. Rem. S., 58, 1125–1128, 1992.

Darracq, A., Greffe, F., Hannerz, F., Destouni, G., and Cvetkovic, V.: Nutrient transport scenarios in a changing Stockholm and Mälaren valley region, Sweden, Water Sci. Technol., 51, 31–38, 2005.

De Wit, M. J. M.: Nutrient fluxes at the river basin scale, I: The Polflow model, Hydrol. Process., 15, 743–759, 2001.

Destouni, G. and Darracq, A.: Nutrient cycling and $N_2O$ emissions in a changing climate: the subsurface water system role, Environ. Res. Lett., 4, 035008, doi:10.1088/1748-9326/4/3/035008, 2009.

Destouni, G., Hannerz, F., Prieto, C., Jarsjö, J., and Shibuo, Y.: Small unmonitored near-coastal catchment areas yielding large mass loading to the sea, Global Biogeochem. Cy., 22, GB4003, doi:10.1029/2008GB003287, 2008.

Destouni, G., Asokan, S. M., and Jarsjö, J.: Inland hydro-climatic interaction: Effects of human water use on regional climate, Geophys. Res. Lett., 37, L18402, doi:10.1029/2010GL044153, 2010.

Farr, T. G., Rosen, P. A., Caro, E., Crippen, R., Duren, R., Hensley, S., Kobrick, M., Paller, M., Rodriguez, E., Roth, L., Seal, D., Shaffer, S., Shimada, J., Umland, J., Werner, M., Oskin, M., Burbank, D., and Alsdorf, D. E.: The shuttle radar topography mission, Rev. Geophys., 45, RG2004, doi:10.1029/2005RG000183, 2007.

Foley, J. A., DeFries, R., Asner, G. P., Barford, C., Bonan, G., Carpenter, S. R., Chapin, F. S., Coe, M. T., Daily, G. C., Gibbs, H. K., Helkowski, J. H., Holloway, T., Howard, E. A., Kucharik, C. J., Monfreda, C., Patz, J. A., Prentice, I. C., Ramankutty, N., and Snyder, P. K.: Global consequences of land use, Science, 309, 570–574, 2005.

Gordon, L. J., Steffen, W., Jönsson, B. F., Folke, C., Falkenmark, M. and Johannessen, Å.: Human modification of global water vapor flows from the land surface, P. Natl. Acad. Sci. USA, 102, 7612–7617, 2005.

Gordon, L. J., Peterson, G. D., and Bennett, E. M.: Agricultural modifications of hydrological flows create ecological surprises, Trends Ecol. Evol., 23, 211–219, 2008.

Groves, D. G., Yates, D., and Tebaldi, C.: Developing and applying uncertain global climate change projections for regional water management planning, Water Resour. Res., 44, W12413, doi:10.1029/2008WR006964, 2008.

IPCC: Climate change 2007: Synthesis report, Contribution of Working Groups I, II and III to the Fourth Assessment Report of the Intergovernmental Panel on Climate Change, 104, 2007.

Jarsjö, J. and Bayer-Raich, M.: Estimating plume degradation rates in aquifers: Effect of propagating measurement and methodological errors, Water Resour. Res., 44, W02501, doi:10.1029/2006WR005568, 2008.

Jarsjö, J. and Destouni, G.: Groundwater discharge into the Aral Sea after 1960, J. Mar. Syst., 47, 109–120, 2004.

Jarsjö, J., Shibuo, Y., and Destouni, G.: Spatial distribution of unmonitored inland water discharges to the sea, J. Hydrol., 348, 59–72, 2008.

Johansson, O., Aimbetov, I., and Jarsjö, J.: Variation of groundwater salinity in the partially irrigated Amudarya River delta, Uzbekistan, J. Mar. Syst., 76, 287–295, 2009.

Keiser, J., De Castro, M. C., Maltese, M. F., Bos, R., Tanner, M., Singer, B. H., and Utzinger, J.: Effect of irrigation and large dams on the burden of malaria on a global and regional scale, Am. J. Trop. Med. Hyg., 72, 392–406, 2005.

Langbein, W. B.: Annual runoff in the United States, US Geological Survey Circular, 52, 1949.

Lee, E., Sacks, W. J., Chase, T. N., and Foley, J. A.: Simulated impacts of irrigation on the atmospheric circulation over Asia, J. Geophys. Res.-Atmos., 116, D08114, doi:10.1029/2010JD014740, 2011.

Lobell, D., Bala, G., Mirin, A., Phillips, T., Maxwell, R., and Rotman, D.: Regional differences in the influence of irrigation on climate, J. Climate, 22, 2248–2255, 2009.

Lobell, D. B. and Field, C. B.: Global scale climate-crop yield relationships and the impacts of recent warming, Environ. Res. Lett., 2, 014002, doi:10.1088/1748-9326/2/1/014002, 2007.

Milly, P. C. D., Wetherald, R. T., Dunne, K. A., and Delworth, T. L.: Increasing risk of great floods in a changing climate, Nature, 415, 514–517, 2002.

Milly, P. C. D., Dunne, K. A., and Vecchia, A. V.: Global pattern of trends in streamflow and water availability in a changing climate, Nature, 438, 347–350, 2005.

Mitchell, T. D. and Jones, P. D.: An improved method of constructing a database of monthly climate observations and associated high-resolution grids, Int. J. Climatol., 25, 693–712, 2005.

Mujumdar, P. P. and Ghosh, S.: Modeling GCM and scenario uncertainty using a possibilistic approach: Application to the Mahanadi River, India, Water Resour. Res., 44, W06407, doi:10.1029/2007WR006137,, 2008.

Palmer, T. N. and Räisänen, J.: Quantifying the risk of extreme seasonal precipitation events in a changing climate, Nature, 415, 512–514, 2002.

Piao, S., Friedlingstein, P., Ciais, P., De Noblet-Ducoudré, N., Labat, D., and Zaehle, S.: Changes in climate and land use have a larger direct impact than rising $CO_2$ on global river runoff trends, P. Natl. Acad. Sci. USA, 104, 15242–15247, 2007.

Radič, V. and Hock, R.: Regionally differentiated contribution of mountain glaciers and ice caps to future sea-level rise, Nat. Geosci., 4, 91–94, 2011.

Rajagopalan, B., Lall, U. and Zebiak, S. E.: Categorical climate forecasts through regularization and optimal combination of multiple GCM ensembles, Mon. Weather Rev., 130, 1792–1811, 2002.

Rakhmatullaev, S., Huneau, F., Kazbekov, J., Le Coustumer, P., Jumanov, J., El Oifi, B., Motelica-Heino, M., and Hrkal, Z.: Groundwater resources use and management in the Amu Darya River Basin (Central Asia), Environ. Earth Sci., 59, 1183–1193, 2010.

Shibuo, Y., Jarsjö, J., and Destouni, G.: Bathymetry-topography effects on saltwater-fresh groundwater interactions around the shrinking Aral Sea, Water Resour. Res., 42, W11410, doi:10.1029/2005WR004207, 2006.

Shibuo, Y., Jarsjö, J., and Destouni, G.: Hydrological responses to climate change and irrigation in the Aral Sea drainage basin, Geophys. Res. Lett., 34, L21406, doi:10.1029/2007GL031465, 2007.

Title Page

Abstract | Introduction

Conclusions | References

Tables | Figures

|◄ | ►|

◄ | ►

Back | Close

Full Screen / Esc

Printer-friendly Version

Interactive Discussion

Siebert, S., Döll, P., Hoogeveen, J., Faures, J.-M., Frenken, K., and Feick, S.: Development and validation of the global map of irrigation areas, Hydrol. Earth Syst. Sci., 9, 535–547, doi:10.5194/hess-9-535-2005, 2005.

Solomon, S., Qin, D., Manning, M., Chen, Z., Marquis, M., Averyt, K. B., Tignor, M., and Miller, H. L.: The Physical Science Basis, Contribution of Working Group I to the Fourth Assessment Report of the Intergovernmental Panel on Climate Change, 2007.

Thornthwaite, C. W.: An approach toward a rational classification of climate, Geogr. Rev., 38, 55–94, 1948.

Törnqvist, R. and Jarsjö, J.: Water Savings Through Improved Irrigation Techniques: Basin-Scale Quantification in Semi-Arid Environments, Water Resour. Manage., doi:10.1007/s11269-011-9819-9, in press, 2011.

Törnqvist, R., Jarsjö, J., and Karimov, B.: Health risks from large-scale water pollution: Trends in Central Asia, Environ. Int., 37, 435–442, 2011.

Turc, L.: Le bilan d'eau des sols: Relations entre les précipitations l'évaporation et l'écoulement, Ann. Agron., 5, 491–595, 1954.

Weiskel, P. K., Vogel, R. M., Steeves, P. A., Zarriello, P. J., DeSimone, L. A., and Ries III, K. G.: Water use regimes: Characterizing direct human interaction with hydrologic systems, Water Resour. Res., 43, W04402, doi:10.1029/2006WR005062,, 2007.

Wisser, D., Fekete, B. M., Vrsmarty, C. J., and Schumann, A. H.: Reconstructing 20th century global hydrography: a contribution to the Global Terrestrial Network-Hydrology (GTN-H), Hydrol. Earth Syst. Sci., 14, 1–24, doi:10.5194/hess-14-1-2010, 2010.

Wood, A. W., Leung, L. R., Sridhar, V., and Lettenmaier, D. P.: Hydrologic implications of dynamical and statistical approaches to downscaling climate model outputs, Climatic Change, 62, 189–216, 2004.

**Table 1.** Number of grid cells within the ASDB for the considered GCMs of IPCCs AR4 and TAR. The IDs of the GCMs are given as in the GCM summary by Solomon et al. (2007).

| ID of GCM | Version | Number of grid cells within ASDB |
|---|---|---|
| CSIRO-CSMK3 | AR4 | 54 |
| ECHAM5-MPEH5 | AR4 | 56 |
| GFDL-GFCM_20_21 | AR4 | 37 |
| HADCM3 | AR4 | 20 |
| NIES-MIMR | AR4 | 24 |
| CNCM3 | AR4 | 24 |
| ECHOG | AR4 | 15 |
| GIER | AR4 | 11 |
| HADGEM | AR4 | 68 |
| INCM3 | AR4 | 7 |
| IPCM4 | AR4 | 19 |
| MRCGCM | AR4 | 23 |
| NCCCSM | AR4 | 99 |
| NCPCM | AR4 | 23 |
| CSIRO-MK2 | TAR | 11 |
| ECHAM4 | TAR | 26 |
| GFDL99-R30 | TAR | 24 |
| HADCM3 | TAR | 20 |
| CCSR/NIES | TAR | 6 |
| CCCma-CGCM2 | TAR | 16 |

**Table 2.** Summary of climate data from observations, ensemble mean results from the 14 AR4 and 6 TAR GCMs, and corresponding hydrological simulation results for the ASDB. Standard deviations are given in parentheses.
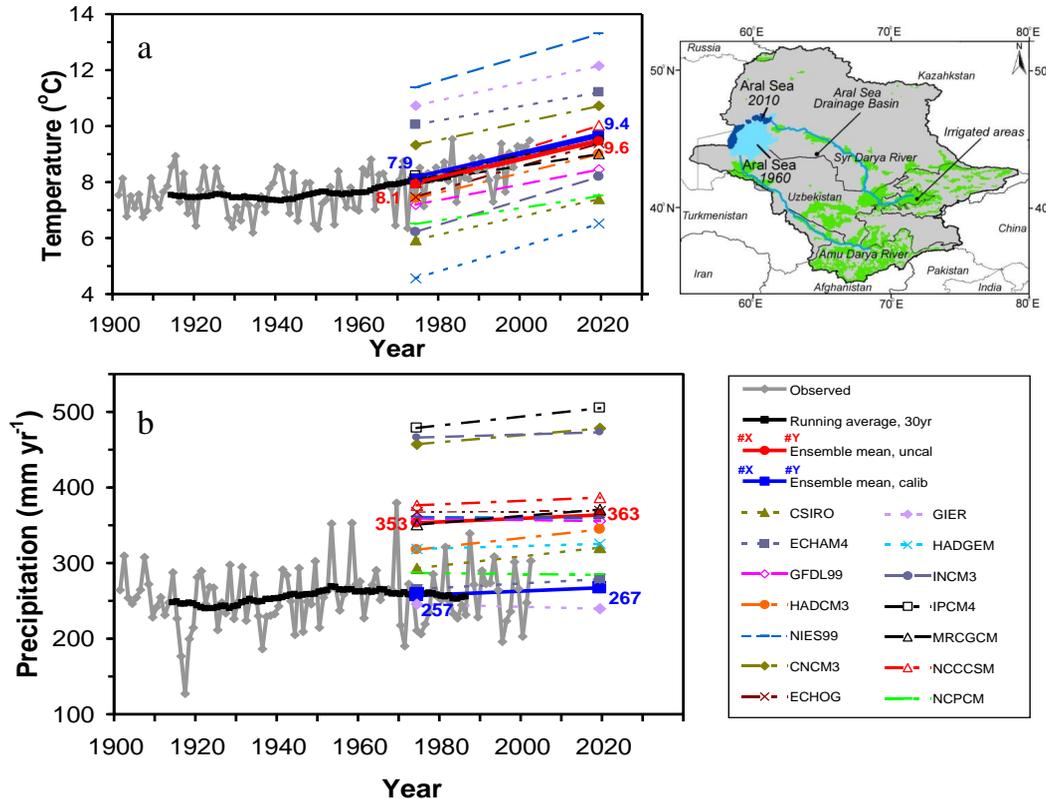
| AR4 | Observed 1961–1990 | GCM mean* 1961–1990, Unal. | GCM mean* 2010–2039, Calibr. | GCM mean* 2010–2039, Uncal. |
|---|---|---|---|---|
| Average $T$ (°C) | 8.1 | 7.9 (1.9) | 9.6 (0.4) | 9.5 (1.9) |
| Total $P$ (km$^3$ yr$^{-1}$) | 481.7 | 670.7 (140) | 501.1 (23.7) | 690.1 (149) |
| *Mean\* from hydrological model* | | | | |
| Export** | 13.4 | 13.4 | 13.4 | 13.4 |
| Total ET (km$^3$ yr$^{-1}$) | 458.2 | 522.3 (76.7) | 482.3 (16.2) | 550.1 (84.9) |
| Total $R$ (km$^3$ yr$^{-1}$) | 10.1 | 135.0 (94.5) | 5.5 (9.3) | 126.7 (99.8) |
| TAR | Observed 1961–1990 | GCM mean* 1961–1990, Uncal. | GCM mean* 2010–2039, Calibr. | GCM mean* 2010–2039, Uncal. |
| Average $T$ (°C) | 8.1 | 7.4 (3.3) | 10.1 (0.4) | 9.4 (3.1) |
| Total $P$ (km$^3$ yr$^{-1}$) | 481.7 | 633.7 (176) | 503.6 (47) | 655.7 (145) |
| *Mean\* from hydrological model* | | | | |
| Export** | 13.4 | 13.4 | 13.4 | 13.4 |
| Total ET (km$^3$ yr$^{-1}$) | 458.2 | 510.7 (120) | 486.5 (33.3) | 549.0 (114) |
| Total $R$ (km$^3$ yr$^{-1}$) | 10.1 | 109.6 (86.7) | 3.8 (15.6) | 94.0 (62.8) |

* Standard deviation in parenthesis.

** Water flow through the Karakum canal and other irrigation canals crossing the ASDB boundary.

Title Page

Abstract | Introduction

Conclusions | References

Tables | Figures

◄ | ►

◄ | ►

Back | Close

Full Screen / Esc

Printer-friendly Version

Interactive Discussion

**Fig. 1.** Observed (grey line; running average in black) and projected (14 AR4 GCMs; colored thin lines) trends in **(a)** temperature $T$, and **(b)** precipitation $P$ for the ASDB. Thick red lines show ensemble mean values of the GCM projections, and thick, blue lines show ensemble mean changes ($\Delta T$ and $\Delta P$) from the observed mean conditions of the reference period 1961–1990. Insert map shows the extent and location of the ASDB (grey area), its irrigated land (green areas), the Aral Sea in 1960 (light blue) and in 2010 (dark blue), and the principal Amu Darya and Syr Darya rivers (blue).

Title Page

Abstract | Introduction
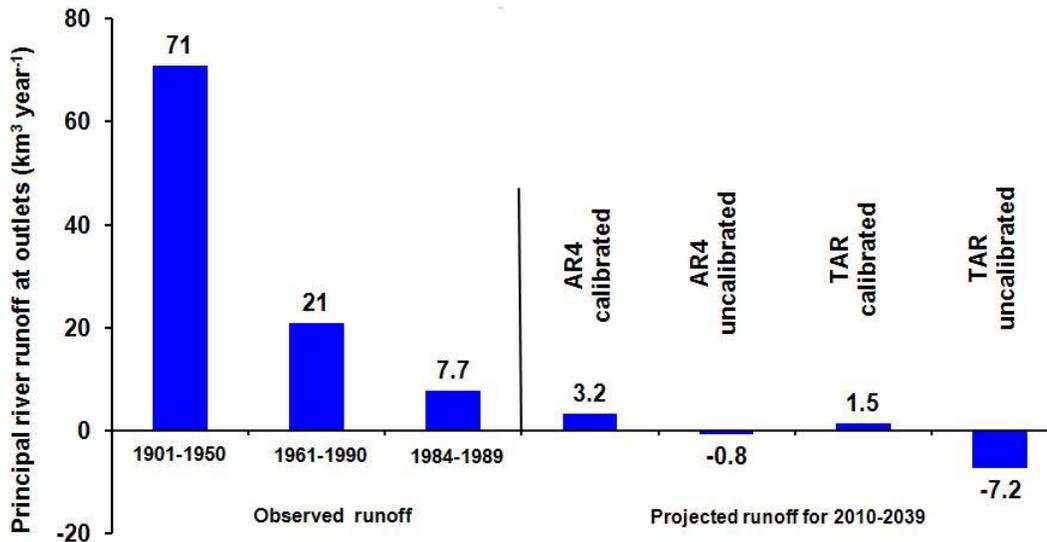
Conclusions | References

Tables | Figures

⏮ | ⏭

◀ | ▶

Back | Close

Full Screen / Esc

Printer-friendly Version

Interactive Discussion

**Fig. 2.** Ensemble mean and standard deviation (error bars) of hydrological model results based on calibrated GCM projections (blue bars) and uncalibrated GCM projections (red bars) of climate change from the reference period 1961–1990 to 2010–2039, based on **(a)** all 14 available GCM projections of AR4, and **(b)** all 6 available GCM projections of TAR.

**Fig. 3.** Observed and projected total runoff of the principal Amu Darya and Syr Darya rivers at their Aral Sea outlets. The observed runoff changes so far are primarily due to irrigation expansion, whereas the future runoff results assume maintained irrigation practices following the 1984–1989 period, and quantify the effect of climate change from the reference period 1961–1990 to 2010–2039, for the same combinations of GCM projections and hydrological modeling methods as in Fig. 2. Negative numbers indicate water depletion upstream of the Aral Sea outlets.
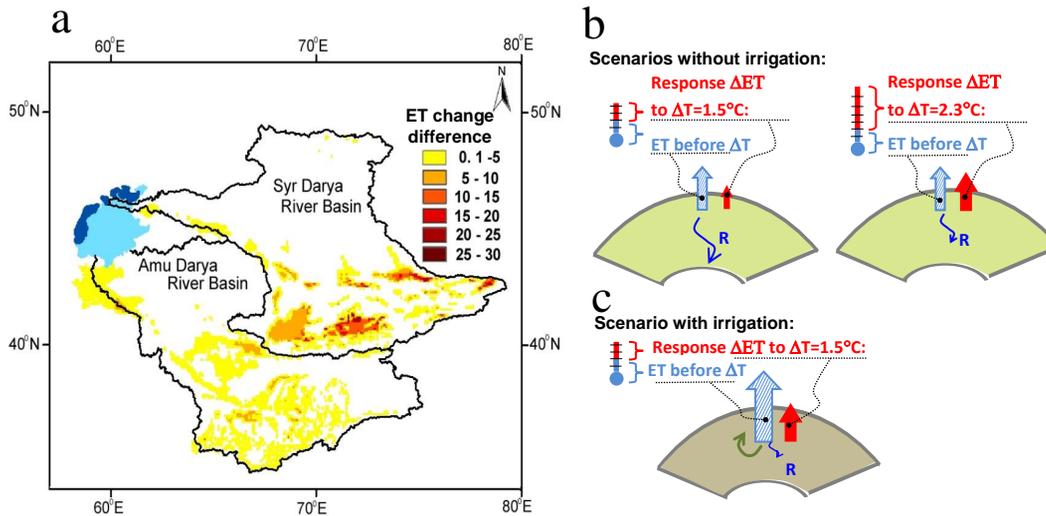
**Fig. 4. (a)** Difference between the irrigation and the non-irrigation scenario results for ET change from the reference period 1961–1990 to 2010–2039. The irrigation induced ET responses are schematically shown with red arrows in: **(b)** for the non-irrigation scenario and temperature increases of 1.5 °C (left panel) and 2.3 °C (right panel), and **(c)** for the irrigation scenario and temperature increase of 1.5 °C.